

# Optimal Control of Load Shedding in Smart Grids

Fu Lin

**Abstract**—We consider the optimal control of load-shedding problem in smart grids where a number of transmission lines are to be taken out of service. The objective is to achieve the minimum interruption of power generation and load at the transmission level, subject to the AC power flow dynamics, the load and generation capacity of the buses, and the phase angle limit across the transmission lines. For this optimal control problem with binary constraints, we show that all decision variables are separable except for the nonlinear power flow equations. We develop an iterative decomposition algorithm, which converts the load shedding problem into a sequence of smaller subproblems. We show that the subproblems are either convex problems that can be solved efficiently or nonconvex problems that have closed-form solutions. Consequently, our algorithm is scalable for large networks. Furthermore, we prove global convergence of our algorithm to a critical point and the objective value is guaranteed to decrease throughout the iterations. Numerical experiments with the IEEE 118-bus test case demonstrate the effectiveness of the developed approach.

**Keywords:** Optimal load shedding, proximal alternating linearization method, power systems, transmission switching.

## I. INTRODUCTION

Redundancy of interconnection in power systems is known to help prevent cascade blackout [1]. On the other hand, recent study suggests that having too much interconnectivity in power networks can result in excessive capacity, which in turn fuels larger blackout [2]. Therefore, a balance between the operational robustness and the network interconnectivity is important for power grid operations.

Traditionally, contingency analysis in power grids has focused on the severity of line outages using linearized power flow models [3]. Recent years have seen vulnerability analysis of line outages using nonlinear power flow models [4]–[6]. The objective of these studies is to identify transmission lines whose removal leads to the maximum damage (e.g., in load shedding) to power systems. The optimal transmission switching is a related line of research that focuses on the switching of transmission lines to reduce congestion in power grids [7], [8].

F. Lin is with the Systems Department, United Technologies Research Center, 411 Silver Ln, East Hartford, CT 06108. E-mail: linf@utrc.utc.com.

While identifying vulnerability in power systems is important, identifying redundancy in power systems is also important [9]. By redundancy, we mean the components (e.g., transmission lines) in the power grid whose removal does not change the grid operation significantly. Suppose that the power grid is operating at its nominal point with a balance between load and power generation. Consider the situation in which the grid operator must temporarily remove a number of transmission lines because of maintenance or security reasons [9]. The change of network topology implies a change of the operating point. Following [4]–[6], we measure the severity of line removal by the amount of load that must be shed. Our objective is to identify a prespecified number of lines whose removal results in minimum load shedding subject to the nonlinear power flow constraints.

We formulate the optimal load-shedding problem, which contains binary decision variables for the on/off lines and the nonlinear AC power flow equations. It falls into the class of mixed-integer nonlinear programs (MINLPs). This challenging optimization problem is beyond the capacities of the state-of-the-art MINLP solvers even for small power systems.

### A. Our Contributions

We summarize our main results.

First, our optimal load shedding model incorporates the AC power dynamics, the generation and load capacities of the buses, and the thermal constraints across the transmission lines. This model allows us to calculate the operating points more accurately than models based on the linearized power flow equations. The resulting optimal control problem is a nonconvex problem due to the AC power flow equations and the binary decision variables for the on/off lines.

Second, we show that all decision variables (i.e., generation, load, phase angles) across buses and transmission lines are separable except for the power flow constraints. This separable structure allows us to develop a decomposition algorithm based on PALM. In particular, PALM decomposes the load shedding problem into a sequence subproblems that are either convex problems or nonconvex problems that have closed-form solutions. As a result, our approach is scalable for large networks.

Third, we prove the global convergence of PALM to a critical point of the nonconvex problem. Furthermore, the objective value is monotonically decreasing throughout

the iterations. Our proof techniques take advantage of recent results in generic alternating methods and the connection with the Kurdyka-Łojasiewicz theory.

In our previous work [10], the alternating direction method of multipliers (ADMM) was proposed to deal with the load shedding problem in DC power networks. The shortcoming of ADMM is that there is no theoretical guarantee of convergence for nonconvex problems. In contrast, PALM allows us to handle nonconvex, nonsmooth problem with provably convergence guarantee.

### B. Literature Review

There is a large body of work on the load shedding problem in smart grids [11]–[20]. We next provide a brief literature review and put our contributions in context.

Several studies focus on the load shedding problem in static networks, that is, the network structure does not change over time [11], [13], [14]. In contrast, our load-shedding model allows the operator to remove a prescribed number of lines and evaluate the minimum amount of load shedding.

Another line of work studies efficient numerical methods for the load shedding problem [12], [16]–[19]. In [12], a discretization technique was developed to convert the differential equations to algebraic constraints. The resulting nonlinear programming (NLP) problem was solved by using standard NLP solvers. Alternatively, conventional optimization methods have been proposed for similar NLP formulations. In [16], the Newton's method was employed to minimize the curtailment of load service after severe faults. In [17], a quasi-Newton method was proposed for the load shedding problem with voltage and frequency characteristics of load. In [18], a projected gradient method was used to solve the under-frequency load shedding problem. In contrast to these NLP-based approaches, our formulation incorporates binary decision variables to model line removals in AC power networks. Thus, it falls in the class of more general class of MINLP problems.

Heuristics approaches have been proposed for the nonconvex load shedding problem [15], [20]. In [15], a particle swarm-based simulated annealing technique was introduced for the under voltage load shedding problem. In [20], tree-like heuristics strategies were proposed for emergency situations to maintain reliability. In contrast to these heuristics approaches with little theoretical guarantees, we prove that PALM converges to a critical point of the nonconvex load shedding problem.

### C. Outline

Our presentation is organized as follows. In Section II, we formulate the optimal load-shedding problem for AC power networks. In Section III, we show the separable

structure of the load-shedding problem. In Section IV, we describe the PALM algorithm and show that each subproblem can be solved efficiently. In Section V, we analyze the convergence behavior of PALM. In Section VI, we provide numerical results for the IEEE test cases. In Section VII, we conclude the paper and discuss future directions.

## II. OPTIMAL LOAD-SHEDDING PROBLEM

In this section, we formulate the optimal load-shedding problem for electrical power grids with AC power flow models. In contrast to existing models in literature that describe AC power flow between individual transmission lines, we take advantage of the incidence matrix to encode the network connection in a matrix form. The compact representation of our model facilitates the derivation of the first-order derivatives and enables the convergence analysis in subsequent sections.

We consider a lossless power network with  $n$  buses and  $m$  lines. A line  $l$  connecting bus  $i$  and bus  $j$  can be described by a vector  $e_l \in \mathbb{R}^n$  with 1 and  $-1$  at the  $i$ th and  $j$ th elements, respectively, and 0 everywhere else. Let  $E = [e_1 \cdots e_m] \in \mathbb{R}^{n \times m}$  be the incidence matrix that describes  $m$  transmission lines of the network, and let  $D \in \mathbb{R}^{m \times m}$  be the diagonal matrix with the  $l$ th diagonal element being the admittance of line  $l$ . For a lossless power grid with fixed voltage at the buses, the active AC power flow equation can be written in a vector form

$$ED \sin(E^T \theta) = P,$$

where  $\theta \in \mathbb{R}^n$  is the phase angles and  $P \in \mathbb{R}^n$  is the real power injection at the buses. Reactive power equation over networks can be written similarly in a vector form. One can extend this model to include per-unit voltages of buses; see [21, Chapter 2.2].

We enumerate the buses such that the power injection  $P$  can be partitioned into a load vector  $P_d \leq 0$  and a generation vector  $P_g > 0$ , thus,  $P = [P_d^T \ P_g^T]^T$ . The sequence of buses indexed in  $P$  is the same as that of the columns of the incidence matrix  $E$ . We assume that the power system is lossless, so the sum of load is equal to the sum of generation

$$\mathbf{1}^T P = 0,$$

where  $\mathbf{1}$  is the vector of all ones.

Let  $\gamma \in \{0, 1\}^m$  denote whether a line is in service or not:  $\gamma_l = 1$  if line  $l$  is in service and  $\gamma_l = 0$  if line  $l$  is out of service. Let  $z = [z_d^T \ z_g^T]^T \in \mathbb{R}^n$ , where  $z_d \geq 0$  and  $z_g \leq 0$  are the load-shedding vector and the generation reduction vector, respectively. It follows that

$$P_d \leq P_d + z_d \leq 0,$$

where the upper bound 0 enforces  $P_d + z_d$  to be a load vector. Similarly, we have

$$0 \leq P_g + z_g \leq P_g,$$

where the lower bound 0 enforces  $P_g + z_g$  to be a generator vector. Since the load shed must be equal to the generation reduction, we have

$$\mathbf{1}^T z = 0.$$

The active power flow equation with possible line removal can be written as

$$ED\text{diag}(\gamma) \sin(E^T \theta) = P + z,$$

where  $\text{diag}(\gamma)$  is a diagonal matrix with its main diagonal equal to  $\gamma$ .

Our objective is to identify a small number of lines in the AC-model power network whose removal will result in the minimum load shedding. Thus, we consider the following *optimal load-shedding* problem:

$$\underset{\gamma, \theta, z}{\text{minimize}} \quad \text{LoadShedding} = \mathbf{1}^T z_d \quad (1a)$$

$$\text{subject to } ED\text{diag}(\gamma) \sin(E^T \theta) = P + z \quad (1b)$$

$$\gamma \in \{0, 1\}^m, \quad m - \mathbf{1}^T \gamma = K \quad (1c)$$

$$\mathbf{1}^T z = 0, \quad z = [z_d^T \ z_g^T]^T \quad (1d)$$

$$0 \leq z_d \leq -P_d, \quad -P_g \leq z_g \leq 0 \quad (1e)$$

$$-\frac{\pi}{2} \leq E^T \theta \leq \frac{\pi}{2}. \quad (1f)$$

The decision variables are the phase angle  $\theta$ , the reduction of load  $z_d$ , the reduction of generation  $z_g$ , and the out-of-service line indicator  $\gamma$ . The problem data are the incidence matrix  $E$  for the network connection, the admittance matrix  $D$  for the transmission lines, the real power injection  $P$  at the buses, and the number of out-of-service lines  $K$ . The angle difference between the buses  $E^T \theta$  takes values between  $-\pi/2$  and  $\pi/2$ .

The adaption of our model to the maximum load-shedding problem is immediate. Our load-shedding problem is based on the model introduced in [4]. Related models have been employed for the contingency analysis in [5] and vulnerability analysis in [6].

### III. SEPARABLE STRUCTURE

The load-shedding problem (1) contains nonlinear constraints and binary variables. One source of nonlinearity is the sinusoidal function and another source is the multiplication between  $\text{diag}(\gamma)$  and  $\sin(E^T \theta)$ . Therefore, it falls into the class of mixed-integer nonlinear programs (MINLPs), which are challenging problems. In particular, finding a feasible point for MINLPs can be computationally expensive or even NP-hard [22]–[24].

The minimum load-shedding problem (1) turns out to have a separable structure that can be exploited. In what follows, we discuss this structure and develop an algorithm based on the proximal alternating linearization method.

A closer look at (1) reveals that the only constraint that couples all decision variables,  $\theta$ ,  $z$ , and  $\gamma$ , is the AC power flow equation (1b). Otherwise, the binary variable,  $\gamma$ , is subject only to the cardinality constraint (1c). The load-shedding and the generation-reduction variables  $z_l$ ,  $z_g$  are subject to the losslessness constraint (1d) and the box constraint (1e). The phase angles of the buses,  $\theta$ , are subject only to the linear inequality constraint (1f). Therefore, the constraints in the load-shedding problem (1) are separable with respect to  $\theta$ ,  $z$ , and  $\gamma$ , provided that the power flow equation (1b) is relaxed.

We next penalize the error in the power flow equation (1b) and include the penalty in the cost function. Let us denote the coupling constraint as

$$c(\gamma, z, \theta) = ED\text{diag}(\gamma) \sin(E^T \theta) - (P + z)$$

and consider

$$\begin{aligned} & \underset{\gamma, z, \theta}{\text{minimize}} \quad H_\rho(\gamma, z, \theta) := \mathbf{1}^T z_d + \frac{\rho}{2} \|c(\gamma, z, \theta)\|_2^2 \\ & \text{subject to } (1c), (1d), (1e), (1f), \end{aligned} \quad (2)$$

where  $\rho$  is a large, positive coefficient. Clearly, (2) is a relaxation of the load-shedding problem (1), since the power flow equation

$$c(\gamma, z, \theta) = 0$$

is no longer enforced. The penalty of the constraint violation is controlled by the positive scalar  $\rho$ . By solving the relaxed problem (2) with a sufficiently large  $\rho$ , the solution of (2) converges to the solution of (1). Additional background on penalty methods can be found in [25, Chapter 13].

### IV. PROXIMAL ALTERNATING LINEARIZATION METHOD

In this section, we develop a proximal alternating linearization method (PALM) that exploits the separable structure of the load-shedding problem. Roughly speaking, PALM minimizes the cost function by cycling through variables in each iteration while keeping other variables fixed. In this alternating minimization approach, the original problem is broken down into a sequence of partial problems that are more amenable to efficient algorithms or even closed-form solutions.

We begin by introducing the following indicator functions of the constraint sets:

$$\phi_1(\gamma) = \begin{cases} 0, & \text{if } \gamma \in \{0, 1\}^m \text{ and } m - \mathbf{1}^T \gamma = K \\ \infty, & \text{otherwise,} \end{cases} \quad (3)$$

$$\phi_2(z) = \begin{cases} 0, & \text{if } \mathbf{0} \leq z_d \leq -P_d \\ & \text{and } -P_g \leq z_g \leq \mathbf{0} \\ & \text{and } \mathbf{1}^T z = 0 \\ \infty, & \text{otherwise,} \end{cases} \quad (4)$$

and

$$\phi_3(\theta) = \begin{cases} 0, & \text{if } -\frac{\pi}{2} \leq E^T \theta \leq \frac{\pi}{2} \\ \infty, & \text{otherwise.} \end{cases} \quad (5)$$

With these indicator functions, the minimization problem (2) can be compactly expressed as

$$\begin{aligned} \underset{\gamma, z, \theta}{\text{minimize}} \quad & \Phi(\gamma, z, \theta) = \phi_1(\gamma) + \phi_2(z) + \phi_3(\theta) \\ & + H_\rho(\gamma, z, \theta). \end{aligned} \quad (6)$$

The PALM algorithm uses the following iterations

$$\gamma^{k+1} \in \underset{\gamma}{\text{argmin}} \left\{ \phi_1(\gamma) + \frac{a_k}{2} \|\gamma - u^k\|_2^2 \right\} \quad (7a)$$

$$z^{k+1} \in \underset{z}{\text{argmin}} \left\{ \phi_2(z) + \frac{b_k}{2} \|z - v^k\|_2^2 \right\} \quad (7b)$$

$$\theta^{k+1} \in \underset{\theta}{\text{argmin}} \left\{ \phi_3(\theta) + \frac{c_k}{2} \|\theta - w^k\|_2^2 \right\}, \quad (7c)$$

where  $a_k$ ,  $b_k$ , and  $c_k$  are positive coefficients. In other words, PALM minimizes  $\Phi$  with respect to  $\gamma$ ,  $z$ , and  $\theta$ , one at a time, while fixing the other variables constant. The quadratic proximal terms penalize the deviation of decision variables  $(\gamma, z, \theta)$  from  $(u^k, v^k, w^k)$

$$\begin{aligned} u^k &= \gamma^k - \frac{1}{a_k} \nabla_\gamma H_\rho(\gamma^k, z^k, \theta^k) \\ v^k &= z^k - \frac{1}{b_k} \nabla_z H_\rho(\gamma^{k+1}, z^k, \theta^k) \\ w^k &= \theta^k - \frac{1}{c_k} \nabla_\theta H_\rho(\gamma^{k+1}, z^{k+1}, \theta^k). \end{aligned} \quad (8)$$

Note that  $(u^k, v^k, w^k)$  is a linear combination of the previous step  $(\gamma^k, z^k, \theta^k)$  and the corresponding partial gradient of  $H_\rho$ . We refer to [26] for extensive discussions on the proximal algorithms and [27] for the generic PALM algorithms.

The minimization problems (7) are projections on the corresponding constraint sets. In particular, the  $z$ -minimization (7b) and the  $\theta$ -minimization problems (7c) are convex problems, whose solutions can be computed efficiently. On the other hand, the  $\gamma$ -minimization (7a) step is a projection on a nonconvex set. It turns out that this nonconvex problem has a closed-form solution.

The  $z$ -minimization problem (7b) can be expressed as

$$\begin{aligned} \underset{z}{\text{minimize}} \quad & \frac{b_k}{2} \|z - v^k\|_2^2 \\ \text{subject to} \quad & L \leq z \leq U, \quad \mathbf{1}^T z = 0, \end{aligned} \quad (9)$$

where the lower bound is  $L = -[\mathbf{0}^T P_g^T]^T$  and the upper bound is  $U = -[P_d^T \mathbf{0}^T]^T$ . The solution of this convex quadratic program with box constraints and a single equality constraint,  $\mathbf{1}^T z = 0$ , can be computed

efficiently (e.g., by using standard solvers such as CVX, CPLEX). The  $\theta$ -minimization problem (7c) can be expressed as

$$\begin{aligned} \underset{\theta}{\text{minimize}} \quad & \frac{c_k}{2} \|\theta - w^k\|_2^2 \\ \text{subject to} \quad & -\frac{\pi}{2} \leq E^T \theta \leq \frac{\pi}{2}. \end{aligned} \quad (10)$$

This bound-constrained least-squares problem can be solved efficiently.

We next provide a closed-form solution to the  $\gamma$ -minimization problem (7a)

$$\begin{aligned} \underset{\gamma}{\text{minimize}} \quad & \frac{a_k}{2} \|\gamma - u^k\|_2^2 \\ \text{subject to} \quad & \gamma \in \{0, 1\}^m, \quad \mathbf{1}^T \gamma = m - K. \end{aligned} \quad (11)$$

**Lemma 1.** Let  $[u^k]_K$  be the  $K$ th smallest element of  $u^k$ . The  $i$ th element of the solution to (11) is given by

$$\gamma_i = \begin{cases} 1 & \text{if } u_i^k \geq [u^k]_K \\ 0 & \text{otherwise,} \end{cases} \quad (12)$$

for  $i = 1, \dots, m$ .

The proof can be found in Appendix A.

Proximal algorithms typically rely on convexity assumptions to guarantee convergence [26]. In contrast, the PALM algorithm does not require the objective or the constraints to be convex. Instead PALM relies on the smoothness assumption of the coupling term  $H_\rho$  and certain Lipschitz conditions of the partial gradients  $\nabla H_\rho$ . Another feature of PALM is that it does not require stepsize rules as in typical descent-based methods. This is because the Lipschitz conditions guarantee the descent of the objective value in each PALM iterate, as discussed in Section V.

To complete the PALM algorithm, we provide the expressions for  $\nabla H_\rho$  and discuss the choice of  $a_k$ ,  $b_k$ , and  $c_k$  in (7).

**Lemma 2.** The partial gradients  $\nabla H_\rho$  with respect to  $\gamma$ ,  $z$ , and  $\theta$  are given by

$$\begin{aligned} \nabla_\gamma H_\rho &= \rho ((DE^T ED) \circ (\sin(E^T \theta) \sin(E^T \theta)^T)) \gamma \\ &\quad - \rho ((\sin(E^T \theta)(P + z)^T ED) \circ I) \mathbf{1}, \end{aligned} \quad (13a)$$

$$\nabla_z H_\rho = [\mathbf{1}^T \mathbf{0}^T]^T + \rho (P + z) - \rho (ED\Gamma \sin(E^T \theta)), \quad (13b)$$

$$\begin{aligned} \nabla_\theta H_\rho &= \rho E \text{diag}(\cos(E^T \theta)) \Gamma D E^T \times \\ &\quad (ED\Gamma \sin(E^T \theta) - (P + z)) \end{aligned} \quad (13c)$$

where  $\circ$  denotes the elementwise product of matrices.

The proof can be found in Appendix B.

The positive coefficients  $a_k$ ,  $b_k$ , and  $c_k$  in (7) and (8) are determined by

$$\begin{aligned} a_k &= r_1 L_1(z^k, \theta^k) \\ b_k &= r_2 L_2(\gamma^{k+1}, \theta^k) \\ c_k &= r_3 L_3(\gamma^{k+1}, z^{k+1}), \end{aligned}$$

**Algorithm 1** Proximal alternating linearization method

---

```

Start with any  $(\gamma^k, z^k, \theta^k)$  and set  $k \leftarrow 0$ .
for  $k = 0, 1, 2, \dots$  until convergence do
  //  $\gamma$ -minimization:
  Set  $a_k = r_1 L_1(z^k, \theta^k)$  where  $r_1 > 1$  and  $L_1$  in (14a). Solve problem (11) via the closed-form expression (12).
  //  $z$ -minimization:
  Set  $b_k = r_2 L_2(\gamma^{k+1}, \theta^k)$  where  $r_2 > 1$  and  $L_2$  in (14b). Solve the convex quadratic problem (9).
  //  $\theta$ -minimization:
  Set  $c_k = r_3 L_3(\gamma^{k+1}, z^{k+1})$  where  $r_3 > 1$  and  $L_3$  in (14c). Solve the convex quadratic problem (10).
end for

```

---

where  $r_i$  for  $i = 1, 2, 3$  are positive constants greater than 1, for example,  $r_i = 2$ . The Lipschitz constants  $L_i$  for the partial gradients  $\nabla H_\rho$  are given by

$$L_1(z^k, \theta^k) = \rho \|(DE^T ED) \circ (\sin(E^T \theta^k) \sin(E^T \theta^k)^T)\| \quad (14a)$$

$$L_2(\gamma^{k+1}, \theta^k) = \rho \quad (14b)$$

$$L_3(\gamma^{k+1}, z^{k+1}) = \rho \|E\|^2 (2\|Q^{k+1}\| + \|R^{k+1}\|) \quad (14c)$$

where  $\|\cdot\|$  denotes the maximum singular value of a matrix. The detailed derivation of  $L_i$  are provided in Section V.

We summarize PALM in Algorithm 1.

## V. CONVERGENCE ANALYSIS

In this section, we show that Algorithm 1 converges to a critical point of the nonconvex loads-shedding problem (2). This convergence behavior is independent of the choice of the initial guess of the decision variables. Furthermore, the objective value  $\Phi$  is monotonically decreasing with the number of iterates, that is,

$$\Phi(\gamma^{k+1}, z^{k+1}, \theta^{k+1}) \leq \Phi(\gamma^k, z^k, \theta^k).$$

We begin with two technical lemmas on the Lipschitz properties of  $\Phi$ .

**Lemma 3.** *The objective function  $\Phi$  in (6) satisfies the following properties:*

- 1)  $\inf_{\gamma, z, \theta} \Phi(\gamma, z, \theta) > -\infty$ ,  $\inf_{\gamma} \phi_1(\gamma) > -\infty$ ,  $\inf_z \phi_2(z) > -\infty$ , and  $\inf_{\theta} \phi_3(\theta) > -\infty$ .
- 2) *For fixed  $(z, \theta)$ , the partial gradient  $\nabla_{\gamma} H_\rho$  is globally Lipschitz, that is,*

$$\|\nabla_{\gamma} H_\rho(\gamma_1, z, \theta) - \nabla_{\gamma} H_\rho(\gamma_2, z, \theta)\| \leq L_1(z, \theta) \|\gamma_1 - \gamma_2\|$$

for all  $\gamma_1$  and  $\gamma_2$ . Likewise, for fixed  $(\gamma, \theta)$ , the partial gradient  $\nabla_z H_\rho$  is globally Lipschitz, that is,

$$\begin{aligned} \|\nabla_z H_\rho(\gamma, z_1, \theta) - \nabla_z H_\rho(\gamma, z_2, \theta)\| &\leq L_2(\gamma, \theta) \|z_1 - z_2\| \end{aligned}$$

for all  $z_1$  and  $z_2$ . For fixed  $(z, \gamma)$ , the partial gradient  $\nabla_{\theta} H_\rho$  is globally Lipschitz, that is,

$$\begin{aligned} \|\nabla_{\theta} H_\rho(\gamma, z, \theta_1) - \nabla_{\theta} H_\rho(\gamma, z, \theta_2)\| &\leq L_3(\gamma, z) \|\theta_1 - \theta_2\| \end{aligned}$$

for all  $\theta_1$  and  $\theta_2$ .

- 3) *There exist positive constants  $s_1, s_2, s_3$  such that*

$$\begin{aligned} \sup_k \{L_1(z^k, \theta^k)\} &\leq s_1, \\ \sup_k \{L_2(\gamma^k, \theta^k)\} &\leq s_2, \\ \sup_k \{L_3(\gamma^k, z^k)\} &\leq s_3. \end{aligned} \quad (15)$$

- 4) *The entire gradient  $\nabla H_\rho(\gamma, z, \theta)$  is Lipschitz continuous on bounded subsets of  $\mathbb{R}^m \times \mathbb{R}^n \times \mathbb{R}^n$ .*

**Remark 1.** Property 1) is necessary for the minimization problems in Algorithm 1, and thus the minimization of  $\Phi$ , to be well defined. Property 2) on the globally Lipschitz bounds is critical for the convergence of PALM. Note that the block Lipschitz property of  $\nabla H_\rho$  is weaker than the globally Lipschitz assumption of  $\Phi$  in joint variables  $(\gamma, z, \theta)$  in standard proximal methods [27]. Property 3) guarantees that the Lipschitz constants for partial gradients are upper bounded by finite numbers. Property 4) is a mild condition which holds when  $H_\rho$  is twice continuously differentiable.

*Proof.* Property 1) is a direct consequence of the non-negativity of  $H_\rho$  and the definition of the indicator functions  $\phi_1$ ,  $\phi_2$ , and  $\phi_3$ . Property 4) holds because  $H_\rho$  is twice continuously differentiable.

To show Property 2), recall that for fixed  $(z^k, \theta^k)$  the Lipschitz constant  $L_1(z^k, \theta^k)$  of  $\nabla_{\gamma} H_\rho$  is determined by

$$\begin{aligned} \|\nabla_{\gamma} H_\rho(\gamma_1, z^k, \theta^k) - \nabla_{\gamma} H_\rho(\gamma_2, z^k, \theta^k)\| &\leq L_1(z^k, \theta^k) \|\gamma_1 - \gamma_2\| \end{aligned}$$

for all  $\gamma_1$  and  $\gamma_2$ . Since  $\nabla_{\gamma} H_\rho$  is an affine function of  $\gamma$  (see (13a)), it follows that

$$L_1(z^k, \theta^k) = \rho \|(DE^T ED) \circ (\sin(E^T \theta^k) \sin(E^T \theta^k)^T)\|.$$

For fixed  $(\gamma^{k+1}, \theta^k)$ , the Lipschitz constant  $L_2(\gamma^{k+1}, \theta^k)$  of  $\nabla_z H_\rho$  is determined by

$$\begin{aligned} \|\nabla_z H_\rho(\gamma^{k+1}, z_1, \theta^k) - \nabla_z H_\rho(\gamma^{k+1}, z_2, \theta^k)\| &\leq L_2(\gamma^{k+1}, \theta^k) \|z_1 - z_2\| \end{aligned}$$

for all  $z_1$  and  $z_2$ . Since  $\nabla_z H_\rho$  is an affine function of  $z$  (see (13b)), it follows that

$$L_2(\gamma^{k+1}, \theta^k) = \rho.$$

For fixed  $(\gamma^{k+1}, z^{k+1})$ , the Lipschitz constant  $L_3(\gamma^{k+1}, z^{k+1})$  of  $\nabla_\theta H_\rho$  is determined by

$$\begin{aligned} \|\nabla_\theta H_\rho(\gamma^{k+1}, z^{k+1}, \theta_1) - \nabla_\theta H_\rho(\gamma^{k+1}, z^{k+1}, \theta_2)\| \\ \leq L_3(\gamma^{k+1}, z^{k+1})\|\theta_1 - \theta_2\| \end{aligned}$$

for all  $\theta_1$  and  $\theta_2$ . The Lipschitz constant for  $\nabla_\theta H_\rho$  is given by (see Appendix C for derivation)

$$L_3(\gamma^k, z^k) = \rho\|E\|^2(2\|Q^k\| + \|R^k\|)$$

where  $\|\cdot\|$  denotes the maximum singular value of a matrix and

$$Q^k = \Gamma^k D E^T E D \Gamma^k, \quad R^k = \Gamma^k D E^T (P + z^k).$$

The proof is complete by establishing Property 3). Since the maximum singular value of Hadamard product of two matrices is bounded by the product of maximum singular values of individual matrices [28, Theorem 5.5.1], it follows that

$$L_1(z^k, \theta^k) \leq \rho\|D E^T E D\| \cdot \|\sin(E^T \theta^k) \sin(E^T \theta^k)^T\|$$

Thus,  $s_1 = \rho m\|D E^T E D\|^2$ . From (14b), we have  $s_2 = \rho$ . From (14c), we have  $s_3 = \rho\|E\|^2\|D E^T E D\|^2(2 + \|P\|)$ .  $\square$

The convergence of PALM relies on the so-called KL property. For detailed discussions on KL theory, we refer to [27] for the references therein. We recall a few definitions needed for our PALM algorithm applied to  $\Phi$ .

**Definition 1.** Let  $f : \mathbb{R}^d \rightarrow (-\infty, +\infty]$  be proper and lower semicontinuous. The function  $f$  is said to have the Kurdyka-Łojasiewicz (KL) property at  $\bar{u} \in \text{dom } \partial f := \{u \in \mathbb{R}^d : \partial f(u) \neq \emptyset\}$  if there exist  $\eta \in (0, +\infty]$ , a neighborhood  $\mathcal{N}$  of  $\bar{u}$ , and a function  $\psi$  such that for all

$$u \in \mathcal{N} \cap \{f(\bar{u}) < f(u) < f(\bar{u}) + \eta\},$$

the following inequality holds:

$$\psi'(f(u) - f(\bar{u})) \cdot \text{dist}(0, \partial f(u)) \geq 1,$$

where  $\text{dist}(x, s) := \inf\{\|y - x\| : y \in s\}$  denotes the distance from a point  $x \in \mathbb{R}^d$  to a set  $s \subset \mathbb{R}^d$ . A function  $f$  is called a KL function if  $f$  satisfies the KL property at each point of  $\text{dom } \partial f$ .

The KL property is a technical condition that controls the difference in function value by the gradient. It turns out that a large class of functions in modern applications satisfy KL property [27]. One useful way of establishing the KL property is via the connection with the semi-algebraic sets and the semi-algebraic functions.

**Definition 2.** A subset  $\mathcal{S}$  of  $\mathbb{R}^d$  is a real semi-algebraic set if there exists a finite number of real polynomial functions  $g_{ij}$  and  $h_{ij} : \mathbb{R}^d \rightarrow \mathbb{R}$  such that

$$\mathcal{S} = \bigcup_{j=1}^p \bigcap_{i=1}^q \{u \in \mathbb{R}^d : g_{ij}(u) = 0 \text{ and } h_{ij}(u) < 0\}.$$

**Definition 3.** A function  $h : \mathbb{R}^d \rightarrow (-\infty, +\infty]$  is called semi-algebraic function if its graph  $\{(u, v) \in \mathbb{R}^{d+1} : h(u) = v\}$  is a semi-algebraic subset of  $\mathbb{R}^{d+1}$ .

With these definitions, we next show the KL property of  $\Phi$ .

**Lemma 4.** The objective function  $\Phi$  in (6) satisfies the Kurdyka-Łojasiewicz (KL) property.

*Proof.* Since  $\Phi$  is the summation of a smooth function  $H_\rho$  and indicator functions  $\phi_1$ ,  $\phi_2$ , and  $\phi_3$  that are lower semicontinuous, it follows that  $\Phi$  is a proper, lower semicontinuous, and semi-algebraic function satisfies the KL property [27, Theorem 3], it suffices to show that  $\Phi$  is semi-algebraic.

To this end, we examine each term in  $\Phi$ . Clearly,  $H_\rho$  is semi-algebraic because it is a real-valued polynomial function. On the other hand,  $\phi_2$  and  $\phi_3$  are indicator functions of semi-algebraic sets; therefore, they are semi-algebraic functions. To show that  $\phi_1$  is semi-algebraic, we note that the binary constraint  $\gamma_i \in \{0, 1\}$  can be expressed as a polynomial equation  $\gamma_i(\gamma_i - 1) = 0$  for  $i = 1, \dots, m$ . Thus, the set  $\{\gamma \mid \gamma \in \{0, 1\}, m - \mathbf{1}^T \gamma = K\}$  is a semi-algebraic set. As a consequence, the indicator function  $\phi_1$  is semi-algebraic. By invoking the property that a finite sum of semi-algebraic functions is also semi-algebraic, we conclude that  $\Phi$  is a semi-algebraic function. This completes the proof.  $\square$

After establishing Lemma 3 and Lemma 4, the main convergence results follow from the pioneering work [27].

**Proposition 1.** Suppose that  $\Phi$  is a KL function that satisfies conditions in Lemma 3. Let  $x^k = (\gamma^k, z^k, \theta^k)$  be a bounded sequence generated by PALM. The following results hold:

- 1) The sequence  $\{x^k\}$  has finite length, that is,

$$\sum_{k=1}^{\infty} \|x^{k+1} - x^k\|_2 < \infty.$$

- 2) The sequence  $\{x^k\}$  converges to a critical point  $x^* = (\gamma^*, z^*, \theta^*)$  of  $\Phi$ .

- 3) The sequence  $\Phi(x^k)$  is nonincreasing,

$$d\|x^{k+1} - x^k\|_2^2 \leq \Phi(x^k) - \Phi(x^{k+1}), \quad k \geq 0$$

where  $d$  is positive constant bounded below.

*Proof.* The finite length property and the convergence to a critical point follow from Theorem 1 in [27]. The monotonicity of the objective value is obtained from Lemma 3 in [27].  $\square$

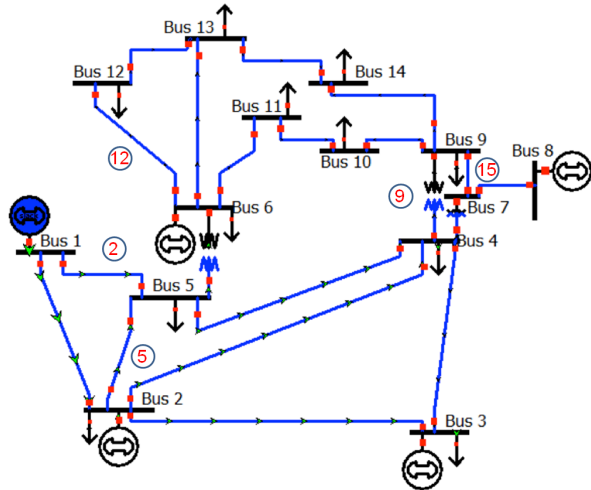


Fig. 1: Diagram of the IEEE 14-bus test case. Five transmission lines,  $\{12, 2, 9, 5, 15\}$ , are to be taken out of service.

TABLE I: Load-shedding strategy for the IEEE 14-bus test case.

$K$	Load Shed	Percentage	Lines Removed
1	51.7003 MW	11.83 %	12
2	65.3584 MW	14.96 %	12, 2
3	110.6711 MW	25.33 %	12, 2, 9
4	214.4981 MW	49.08 %	12, 2, 9, 5
5	277.3910 MW	63.48 %	12, 2, 9, 5, 15

## VI. NUMERICAL RESULTS

In this section, we verify that the convergence results of PALM and study its solution quality via two test cases.

### A. IEEE 14-bus Test Case

Consider the IEEE 14-bus test case shown in Fig. 1. This system has 5 generator buses, 9 load buses, and 20 transmission lines. We compute the generation profile  $P_g$  and the load profile  $P_d$  by solving the steady-state power flow equations via MATPOWER [29].

Figure 2 shows the convergence results of PALM. The objective function, the dual residuals, and the primal residual all decrease monotonically with the PALM iterates, thereby confirming the prediction in Proposition 1. The convergence of PALM is most significant in the first 100 iterates, in this case. Afterwards, the convergence rate of PALM becomes linear. This linear rate depends on the size of the problem and the choice of parameter  $\rho$ . While a bigger  $\rho$  improves primal convergence rate, it slows down the dual convergence rate. In practice, we find that  $\rho \in [10^4, 10^6]$  achieves a good balance between the primal and dual residuals.

We take out up to 5 lines to see the progress of the load shedding in this small network. As the out-of-service

number of lines increases from  $K = 1$  to  $K = 5$ , the amount of load shed increases from 11.83% to 63.48% of the total power load; see Table I.

The set of lines to be taken out of service is a subset of the lines as  $K$  increases. This implies consistency in the set of optimal transmission lines for load-shedding. It is worth mentioning that PALM is initialized with  $(\gamma = 1, \theta = 0, z = 0)$  for all  $K = 1, \dots, 5$ . In other words, there is no prior information to suggest a stable set of optimal lines. The out-of-service lines are highlighted in Fig. 1.

### B. IEEE 118-bus Test Case

We next consider the IEEE 118-bus test case as shown in Fig. 3. This large power system has 54 generator buses, 64 load buses, and 186 transmission lines. The generation profile  $P_g$  and load profile  $P_d$  are obtained by solving the steady-state power flow equations via MATPOWER [29].

While the 118-bus system is much larger than the 14-bus system, the convergence behavior of PALM is quite similar. In particular, the objective value, the dual residuals, and the primal residual all decrease monotonically; see Fig. 4. The convergence rate does not seem to be linear for this large problem. In 3000 PALM iterates, the primal residual is smaller than  $10^{-3}$  and the dual residual is smaller than  $10^{-6}$ . It is worth mentioning that the computational time is less than 10 minutes on a laptop with 8GB RAM running 2.4GHz CPU.

Table II shows the load-shedding strategy identified for up to 5 transmission lines. As observed in 14-bus test case, the optimal set of lines to be taken out of service is a subset of lines when  $K$  is increased. For this large system, the load shed percentage is within 1.5% when 5 lines are taken out. This is in contrast to the 14-bus system, in which the load shed percentage is 64% when  $K = 5$ .

To gain some insight into the out-of-service lines, we consider the types of buses with which the lines connect. Table III shows a total of 5 lines and 10 buses, among which 3 buses are load buses and 7 buses are generator buses. In other words, 4 out of 5 lines are between a generator bus and a load bus.

We next consider the phase angle across transmission lines. A larger phase angle implies a larger power transfer over a transmission line. Thus, it is a good indicator of overload in contingency analysis of power grids [4]. Figure 5 shows the phase angle difference  $E^T \theta$  across all 186 lines when lines  $\{174, 119, 110, 135, 120\}$  are taken out of services. The maximum angle difference is less than 2.5 degrees. In particular, 85% of the phase angles are less than 0.5 degrees, indicating a well-balanced operating status.

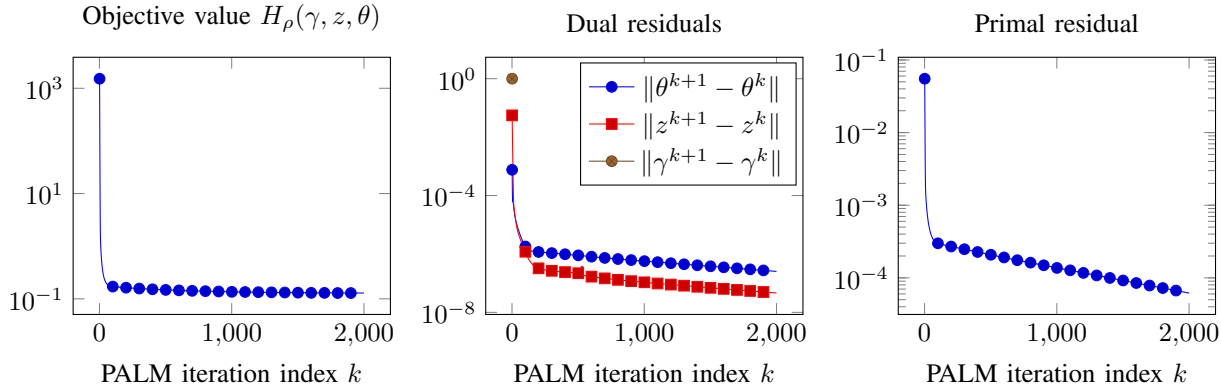


Fig. 2: Convergence results of PALM for the IEEE 14-bus test case: the objective value (left), the dual residuals (middle), and the primal residual (right). The markers show at every 100 iterates.

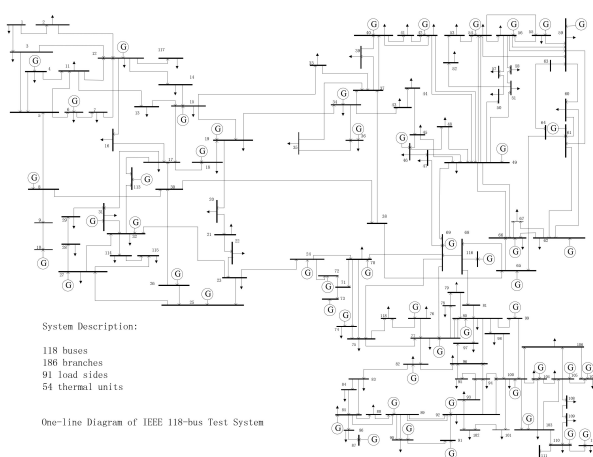


Fig. 3: Diagram of the IEEE 118-bus test case.

TABLE II: Load-shedding strategy for the IEEE 118-bus test case.

K	Load Shed	Percentage	Lines Removed
1	28.02 MW	0.6404 %	174
2	38.86 MW	0.8882 %	174, 119
3	42.49 MW	0.9712 %	174, 119, 110
4	56.37 MW	1.2886 %	174, 119, 110, 135
5	58.01 MW	1.3258 %	174, 119, 110, 135, 120

TABLE III: The set of out-of-service lines and the bus types for the IEEE 118-bus test case.

Line	Bus	Type	Bus	Type
110	70	generator	71	load
119	69	generator	77	generator
120	75	load	77	generator
135	85	generator	88	load
174	103	generator	110	generator

## VII. CONCLUSIONS

We formulate the minimum load-shedding problem for AC power networks. We show that this nonconvex optimal control problem has a separable structure that can be exploited by PALM. This algorithm decomposes load-shedding problem into a sequence of subproblems that are amenable to convex optimization and closed-form solutions. We prove convergence of PALM to a critical point by leveraging KL theory.

We believe that our proof techniques and the upper bounds on the Lipschitz constants can be instrumental in developing other decomposition algorithms in large-scale power networks. While our model focuses on active AC power flows, the dynamics for the reactive power flows can be captured by the same set of nonlinear equations. We anticipate that the developed approach can be applied to fully nonlinear models with both active and reactive power equations.

## APPENDIX

### A. Proof of Lemma 1

We prove by contradiction. Let  $\gamma$  satisfy  $\mathbf{1}^T \gamma = m - K$  and  $\gamma_i \in \{0, 1\}$ , but  $\gamma$  is different from the projection in (12). In other words, there exists at least one element of  $\gamma$ , say, the  $l$ th element such that  $\gamma_l = 1$  with the corresponding  $u_l^k < [u^k]_K$ , and at least one element, say, the  $j$ th element such that  $\gamma_j = 0$  with the corresponding  $u_j^k \geq [u^k]_K$ . Consider

$$\delta_{lj} = (\gamma_l - u_l^k)^2 + (\gamma_j - u_j^k)^2 = (1 - u_l^k)^2 + (u_j^k)^2.$$

and the cost of the swapping the values of  $\gamma_l$  and  $\gamma_j$

$$\delta_{jl} = (u_l^k)^2 + (1 - u_j^k)^2.$$

Since  $\delta_{lj} - \delta_{jl} = 2(u_j^k - u_l^k) > 0$ , we conclude that the cost function decreases if we choose  $(\gamma_l = 0, \gamma_j = 1)$  instead of  $(\gamma_l = 1, \gamma_j = 0)$ . In other words, we can

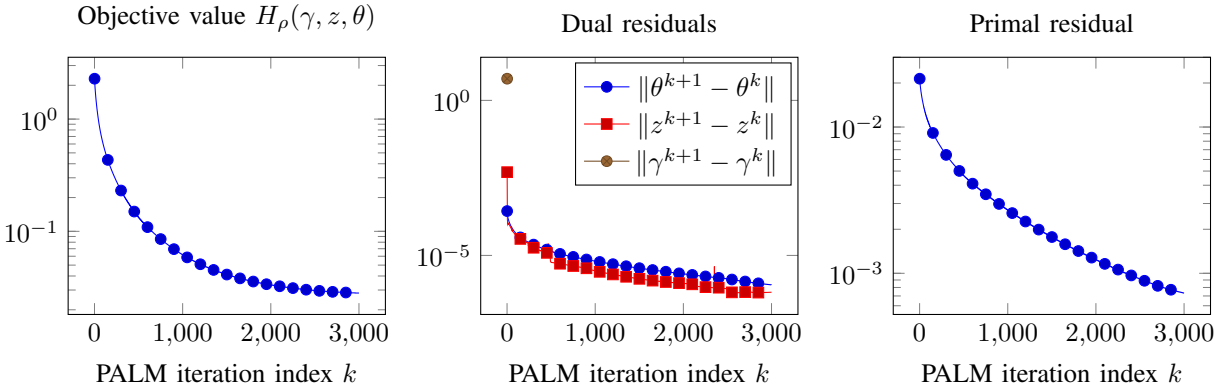


Fig. 4: Convergence results of PALM for the IEEE 118-bus test case: the objective value (left), the dual residuals (middle), and the primal residual (right). The markers show at every 100 iterates.

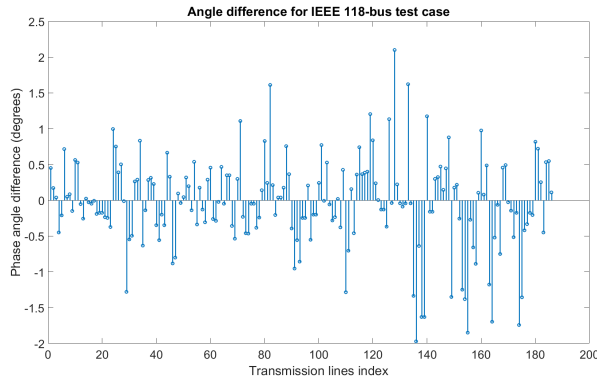


Fig. 5: The phase angle across transmission lines after 5 lines,  $\{174, 119, 110, 135, 120\}$ , are taken out of service for the 118-bus system.

reduce the cost by swapping the values of  $\gamma_l = 1$  with respect to  $u_l^k < [u^k]_K$  and  $\gamma_j = 0$  with respect to  $u_l^k \geq [u^k]_K$  until (12) is satisfied for all elements of  $\gamma$ . This completes the proof.

### B. Proof of Lemma 2

The derivations of (13a) and (13b) are straightforward, as they amount to taking the derivatives of quadratic functions, thus omitted. The derivation of (13c) involves taking the first-order variation for sine and cosine functions. We begin by taking variation  $\tilde{\theta}$  around  $\theta$

$$\begin{aligned} \sin(E^T(\theta + \tilde{\theta})) &= \sin(E^T\theta) \circ \cos(E^T\tilde{\theta}) \\ &\quad + \cos(E^T\theta) \circ \sin(E^T\tilde{\theta}) \end{aligned}$$

where  $\circ$  is the Hadamard (elementwise) product. When  $\tilde{\theta}$  is small, we have the first-order approximation

$$\sin(E^T(\theta + \tilde{\theta})) \approx \sin(E^T\theta) + \text{diag}(\cos(E^T\theta))E^T\tilde{\theta}.$$

It follows that the first-order approximation of  $H_\rho(\theta + \tilde{\theta})$  is given by

$$\begin{aligned} H_\rho(\theta + \tilde{\theta}) &\approx H_\rho(\theta) + \rho (ED\Gamma \sin(E^T\theta) - (P + z))^T \\ &\quad \times ED\Gamma \text{diag}(\cos(E^T\theta))E^T\tilde{\theta}. \end{aligned}$$

Taking the transpose of the matrix multiplying  $\tilde{\theta}$  yields

$$\nabla_\theta H_\rho(\theta) = \rho E \text{diag}(\cos(E^T\theta)) [Q \sin(E^T\theta) - R].$$

where  $Q = \Gamma D E^T E D \Gamma$  and  $R = \Gamma D E^T (P + z)$ .

### C. Lipschitz constant of $\nabla_\theta H_\rho$

Recall that

$$\|\sin(\theta_1 - \theta_2)\| \leq \|\theta_1 - \theta_2\|$$

for all  $\theta_1, \theta_2$ . We have

$$\begin{aligned} &\|\sin(E^T\theta_1) - \sin(E^T\theta_2)\| \\ &= \|2 \cos(E^T(\theta_1 + \theta_2)/2) \circ \sin(E^T(\theta_1 - \theta_2)/2)\| \\ &\leq 2 \|\sin(E^T(\theta_1 - \theta_2)/2)\| \leq \|E\| \|\theta_1 - \theta_2\|. \end{aligned} \quad (16)$$

The first equality is the elementwise sum-to-product identity and the first inequality follows from the fact that all cosine functions are upper bounded by 1. Similar calculation yields

$$\|\cos(E^T\theta_1) - \cos(E^T\theta_2)\| \leq \|E\| \|\theta_1 - \theta_2\|. \quad (17)$$

Let  $f(\theta) = \sin(E^T\theta)$  and  $g(\theta) = \text{diag}(\cos(E^T\theta))Q$ . By adding and subtracting the same term yields

$$\begin{aligned} &g(\theta_1)f(\theta_1) - g(\theta_2)f(\theta_2) \\ &= g(\theta_1)(f(\theta_1) - f(\theta_2)) + (g(\theta_1) - g(\theta_2))f(\theta_2). \end{aligned}$$

We calculate

$$\begin{aligned} &\|g(\theta_1)f(\theta_1) - g(\theta_2)f(\theta_2)\| \\ &\leq \|\text{diag}(\cos(E^T\theta_1))Q(\sin(E^T\theta_1) - \sin(E^T\theta_2))\| \\ &\quad + \|\text{diag}(\cos(E^T\theta_1) - \cos(E^T\theta_2))Q \sin(E^T\theta_2)\| \\ &\leq 2\|Q\| \|E\| \|\theta_1 - \theta_2\| \end{aligned}$$

where we have used (16) and (17). It follows that the Lipschitz constant for  $\nabla_{\theta} H_{\rho}$  is given by

$$\|\nabla_{\theta} H_{\rho}(\theta_1) - \nabla_{\theta} H_{\rho}(\theta_2)\| \leq L_3(\gamma^{k+1}, z^{k+1})\|\theta_1 - \theta_2\|,$$

where

$$L_3(\gamma^{k+1}, z^{k+1}) = \rho\|E\|^2(2\|Q^{k+1}\| + \|R^{k+1}\|)$$

and

$$\begin{aligned} Q^{k+1} &= \Gamma^{k+1} D E^T E D \Gamma^{k+1}, \\ R^{k+1} &= \Gamma^{k+1} D E^T (P + z^{k+1}). \end{aligned}$$

## REFERENCES

- [1] G. Andersson, P. Donalek, R. Farmer, N. Hatziargyriou, I. Kamwa, P. Kundur, N. Martins, J. Paserba, P. Pourbeik, J. Sanchez-Gasca *et al.*, "Causes of the 2003 major grid blackouts in North America and Europe, and recommended means to improve system dynamic performance," *IEEE Transactions on Power Systems*, vol. 20, no. 4, pp. 1922–1928, 2005.
- [2] C. D. Brummitt, R. M. D'Souza, and E. Leicht, "Suppressing cascades of load in interdependent networks," *Proceedings of the National Academy of Sciences*, vol. 109, no. 12, pp. E680–E689, 2012.
- [3] F. D. Galiana, "Bound estimates of the severity of line outages in power system contingency analysis and ranking," *IEEE Transactions on Power Apparatus and Systems*, no. 9, pp. 2612–2624, 1984.
- [4] V. Donde, V. López, B. Lesieutre, A. Pinar, C. Yang, and J. Meza, "Identification of severe multiple contingencies in electric power networks," in *Proceedings of the 37th Annual North American Power Symposium*, 2005, pp. 59–66.
- [5] ———, "Severe multiple contingency screening in electric power systems," *IEEE Transactions on Power Systems*, vol. 23, no. 2, pp. 406–417, 2008.
- [6] A. Pinar, J. Meza, V. Donde, and B. Lesieutre, "Optimization strategies for the vulnerability analysis of the electric power grid," *SIAM Journal on Optimization*, vol. 20, no. 4, pp. 1786–1810, 2010.
- [7] K. W. Hedman, R. P. O'Neill, E. B. Fisher, and S. S. Oren, "Optimal transmission switching with contingency analysis," *IEEE Transactions on Power Systems*, vol. 24, no. 3, pp. 1577–1586, 2009.
- [8] M. Khanabadi, H. Ghasemi, and M. Doostizadeh, "Optimal transmission switching considering voltage security and N-1 contingency analysis," *IEEE Transactions on Power Systems*, vol. 28, no. 1, pp. 542–550, 2013.
- [9] F. Li, W. Qiao, H. Sun, H. Wan, J. Wang, Y. Xia, Z. Xu, and P. Zhang, "Smart transmission grid: Vision and framework," *IEEE Transactions on Smart Grid*, vol. 1, no. 2, pp. 168–177, 2010.
- [10] F. Lin and C. Chen, "An ADMM algorithm for load shedding in electric power grids," in *The Proceedings of the 2016 American Control Conference*, 2016, pp. 5002–5007.
- [11] M. Mostafa, M. El-Hawary, G. Mbamalu, M. Mansour, K. El-Nagar, and A. El-Araby, "A computational comparison of steady state load shedding approaches in electric power systems," *IEEE Transactions on Power Systems*, vol. 12, no. 1, pp. 30–37, 1997.
- [12] D. Xu and A. A. Girgis, "Optimal load shedding strategy in power systems with distributed generation," in *Power Engineering Society Winter Meeting*, vol. 2, 2001, pp. 788–793.
- [13] E. E. Aponte and J. K. Nelson, "Time optimal load shedding for distributed power systems," *IEEE Transactions on Power Systems*, vol. 21, no. 1, pp. 269–277, 2006.
- [14] R. Faranda, A. Pievatolo, and E. Tironi, "Load shedding: a new proposal," *IEEE Transactions on Power Systems*, vol. 22, no. 4, pp. 2086–2093, 2007.
- [15] N. Sadati, T. Amraee, and A. Ranjbar, "A global particle swarm-based-simulated annealing optimization technique for under-voltage load shedding problem," *Applied Soft Computing*, vol. 9, no. 2, pp. 652–657, 2009.
- [16] L. P. Hajdu, J. Peschon, W. F. Tinney, and D. Piercy, "Optimum load-shedding policy for power systems," *IEEE Transactions on Power Apparatus and Systems*, no. 3, pp. 784–795, 1968.
- [17] K. Palaniswamy, J. Sharma, and K. Misra, "Optimum load shedding taking into account of voltage and frequency characteristics of loads," *IEEE Transactions on Power Apparatus and Systems*, no. 6, pp. 1342–1348, 1985.
- [18] Y. Halevi and D. Kottick, "Optimization of load shedding system," *IEEE Transactions on Energy Conversion*, vol. 8, no. 2, pp. 207–213, 1993.
- [19] V. V. Terzija, "Adaptive underfrequency load shedding based on the magnitude of the disturbance estimation," *IEEE Transactions on Power Systems*, vol. 21, no. 3, pp. 1260–1266, 2006.
- [20] S. Pahwa, C. Scoglio, S. Das, and N. Schulz, "Load-shedding strategies for preventing cascading failures in power grid," *Electric Power Components and Systems*, vol. 41, no. 9, pp. 879–895, 2013.
- [21] E. Scholtz, "Observer-based monitors and distributed wave controllers for electromechanical disturbances in power systems," Ph.D. dissertation, Massachusetts Institute of Technology, 2004.
- [22] R. Fletcher and S. Leyffer, "Solving mixed-integer nonlinear programs by outer approximation," *Mathematical Programming*, vol. 66, no. 1-3, pp. 327–349, 1994.
- [23] S. Leyffer, "Integrating SQP and branch-and-bound for mixed-integer nonlinear programming," *Computational Optimization and Applications*, vol. 18, no. 3, pp. 295–309, 2001.
- [24] K. Abhishek, S. Leyffer, and J. Linderoth, "FILMINT: An outer approximation-based solver for convex mixed-integer nonlinear programs," *INFORMS Journal on Computing*, vol. 22, no. 4, pp. 555–567, 2010.
- [25] D. G. Luenberger and Y. Ye, *Linear and nonlinear programming*. Springer, 2008.
- [26] N. Parikh and S. P. Boyd, "Proximal algorithms," *Foundations and Trends in optimization*, vol. 1, no. 3, pp. 127–239, 2014.
- [27] J. Bolte, S. Sabach, and M. Teboulle, "Proximal alternating linearized minimization for nonconvex and nonsmooth problems," *Mathematical Programming*, vol. 146, no. 1-2, pp. 459–494, 2014.
- [28] R. A. Horn and C. R. Johnson, "Topics in matrix analysis," 1991.
- [29] R. D. Zimmerman, C. E. Murillo-Sánchez, and R. J. Thomas, "MATPOWER: Steady-state operations, planning, and analysis tools for power systems research and education," *IEEE Transactions on Power Systems*, vol. 26, no. 1, pp. 12–19, 2011.